AGU ADVANCING EARTH AND SPACE SCIENCE

Geophysical Research Letters

RESEARCH LETTER
10.1029/2020GL090260

Special Section:
The COVID-19 Pandemic: Linking Health, Society, and Environment

Enhanced $PM_{2.5}$ Decreases and O_3 Increases in China During COVID-19 Lockdown by Aerosol-Radiation Feedback

Jia Zhu[1], Lei Chen[1,2], Hong Liao[1], Hao Yang[1], Yang Yang[1], and Xu Yue[1]

[1]Jiangsu Key Laboratory of Atmospheric Environment Monitoring and Pollution Control, Jiangsu Collaborative Innovation Center of Atmospheric Environment and Equipment Technology, School of Environmental Science and Engineering, Nanjing University of Information Science & Technology, Nanjing, China, [2]Key Laboratory of Meteorological Disaster, Ministry of Education, Joint International Research Laboratory of Climate and Environment Change, Collaborative Innovation Center on Forecast and Evaluation of Meteorological Disasters, Nanjing University of Information Science & Technology, Nanjing, China

Key Points:

- Emission reduction due to COVID-19 lockdown induces $PM_{2.5}$ decrease by 16.3 μg m^{-3} (O_3 increase by 10.2 ppbv) over North China Plain
- Aerosol-radiation feedback enhances emission-reduction-induced $PM_{2.5}$ decrease by 16.6% (O_3 increase by 7.8%) during COVID-19 lockdown
- The enhancement of $PM_{2.5}$ decline (O_3 rise) is ascribed to aerosol chemistry process (physical advection and vertical mixing processes)

Supporting Information:

- Supporting Information S1

Correspondence to:
H. Liao and L. Chen,
hongliao@nuist.edu.cn;
chenlei@nuist.edu.cn

Citation:
Zhu, J., Chen, L., Liao, H., Yang, H., Yang, Y., & Yue, X. (2021). Enhanced $PM_{2.5}$ decreases and O_3 increases in China during COVID-19 lockdown by aerosol-radiation feedback. *Geophysical Research Letters*, *48*, e2020GL090260. https://doi.org/10.1029/2020GL090260

Received 13 AUG 2020
Accepted 19 NOV 2020

Abstract We apply an online-coupled meteorology-chemistry model (WRF-Chem) embedded with an improved process analysis to examine aerosol-radiation feedback (ARF) impacts on effectiveness of emission control due to Coronavirus Disease 2019 (COVID-19) lockdown over North China Plain. Emission reduction alone induces $PM_{2.5}$ decrease by 16.3 μg m^{-3} and O_3 increase by 10.2 ppbv during COVID-19 lockdown. The ARF enhances $PM_{2.5}$ decrease by 2.7 μg m^{-3} (16.6%) and O_3 increase by 0.8 ppbv (7.8%). The ARF-induced enhancement of $PM_{2.5}$ decline is mostly attributed to aerosol chemistry process, while enhancement of O_3 rise is ascribed to physical advection and vertical mixing processes. A set of sensitivity experiments with emission reductions in different degrees indicate that the ARF-induced enhancements of $PM_{2.5}$ declines (O_3 rises) follow a robust linear relationship with the emission-reduction-induced $PM_{2.5}$ decreases. The fitted relationship has an important implication for assessing the effectiveness of emission abatement at any extent.

Plain Language Summary Efforts to inhibit the spread of Coronavirus Disease 2019 (COVID-19) remarkably lowered social-economic activities over China during January–February 2020. Observational evidence indicated moderate $PM_{2.5}$ decreases and undesirable O_3 increases during COVID-19 lockdown. It is known that aerosols can influence air quality via aerosol-radiation feedback (ARF). Therefore, it is of great interest to explore how ARF affects the responses of $PM_{2.5}$ and O_3 air quality to emission reduction due to COVID-19 lockdown. Our study shows that ARF enhances emission-reduction-induced $PM_{2.5}$ decrease by 16.6% and O_3 increase by 7.8% during COVID-19 lockdown. The fitted linear relationship between emission-reduction-induced $PM_{2.5}$ decreases and ARF-induced enhancements of $PM_{2.5}$ declines (O_3 rises) has an important implication for evaluating the effectiveness of emission mitigation in any degree.

1. Introduction

Aerosols can perturb the radiative balance of the atmosphere and surface by directly scattering and absorbing solar radiation (direct radiative effect), or indirectly serving as cloud condensation nucleus and then altering cloud properties (indirect radiative effect) (J. Gao et al., 2018; Z. Li, Guo, et al., 2017; J. Li, Han, et al., 2019; Z. Li, Rosenfeld, et al., 2017; B. Zhao et al., 2017). The perturbed radiative balance induces changes in a set of meteorological variables (e.g., temperature, relative humidity, wind, and planetary boundary layer height), and further exert feedbacks on air quality by altering physical and chemical process (J. Li et al., 2020; Lou et al., 2017, 2019; Petaja et al., 2016; Yang et al., 2017), which is known as aerosol-radiation feedback (ARF hereafter).

The positive effects of ARF on fine particulate matter ($PM_{2.5}$) have been identified by extensive studies (Chen et al., 2019; Y. Gao et al., 2015; Huang et al., 2018; Liu et al., 2018; Su et al., 2018). Aerosols exert a substantial positive radiative forcing (and therefore heating) in the atmosphere but a remarkable negative radiative forcing (and therefore cooling) at the surface, leading to a decrease in surface-layer wind speed and suppression of planetary boundary layer (PBL) development (Huang et al., 2018; Su et al., 2018). Both lower

wind speed and PBL height (PBLH) facilitate more stable atmosphere and in turn increase surface-layer $PM_{2.5}$ levels (Chen et al., 2019; Qiu et al., 2017). The decreased PBLH and surface temperature can also increase surface relative humidity, and therefore, accelerate formation of surface particulates via heterogeneous reactions and hygroscopic growth, exacerbating haze pollution (Liu et al., 2018).

The manifestations of ARF impacts on another important air pollutant, ozone (O_3), include changes in photolysis rates and atmospheric dynamics (Tian et al., 2019; W. Wang et al., 2019; Xing et al., 2017). The reductions in solar radiation owing to aerosols result in lower photolysis rates and less O_3 generation (Tian et al., 2019; W. Wang et al., 2019; Zhu et al., 2019). The changes in aerosol-induced atmospheric ventilation and rainfall may also influence O_3 concentrations. The changes in atmospheric dynamics due to aerosols lead to O_3 decreases in winter but increases in summer (Xing et al., 2017).

Since aerosols influence meteorological conditions and further air quality through ARF, it is of great interest to explore how ARF affects the responses of air quality to emission control, which is a tendency to improve air quality. Emission reduction leads to changes in aerosols, which impacts meteorological conditions and further air quality ($PM_{2.5}$ and O_3). Limited studies reported how aerosol-radiation interactions impacted the effectiveness of emission abatement for $PM_{2.5}$ pollution (M. Gao et al., 2017; W. Wen, Guo, et al., 2020; Xing et al., 2015; Zhou et al., 2019). The effects of ARF on O_3 responses to emission mitigation, however, are totally unknown. What's more, the prominent physical or chemical processes responsible for ARF impacts remain largely elusive.

Efforts to inhibit the spread of Coronavirus Disease 2019 (COVID-19), e.g., the implements of nationwide restrictions on population movement (lockdown), have remarkably lowered social-economic activities and reduced anthropogenic emissions over China during January–February 2020, which happens to provide an opportunity to investigate how ARF impacts $PM_{2.5}$ and O_3 responses to emission control. Recent studies have reported significant NO_2 reductions, moderate $PM_{2.5}$ decreases, and undesirable O_3 increases during COVID-19 outbreak (Huang et al., 2020; Shi & Brasseur, 2020; P. Wang et al., 2020; Y. Zhao et al., 2020).

We examine the ARF effects on $PM_{2.5}$ and O_3 responses to emission reduction during COVID-19 lockdown, by using a fully online (two-way) coupled meteorology-chemistry model. An improved online integrated process rate (IPR) analysis scheme (i.e., process analysis) is developed in the model to explore how each physical/chemical process acts on the ARF impacts. This study focuses on $PM_{2.5}$ and O_3 air quality over North China Plain (NCP) of China from January 23 to February 29, 2020 when strict limitations on human activities to control COVID-19 spread were implemented. The study is believed to exert a novel contribution to understand the effectiveness of emission abatement.

2. Materials and Methods

2.1. Observation Description

The study region overlaid with meteorological and environmental monitoring sites is shown in Figure S1a. The analyzed region NCP in this study covers six provinces, including Beijing-Tianjin-Hebei-Shandong-Shanxi-Henan. Sources of meteorological and environmental measurements are described in Text S1. Figures S1b and S1c exhibit observed daily $PM_{2.5}$ and O_3 concentrations averaged over NCP before (January 1–22, 2020) and during (January 23–February 29, 2020) the COVID-19 lockdown period. The observed $PM_{2.5}$ concentration is 103.2 $\mu g\ m^{-3}$ before COVID-19 lockdown and decreases to 69.8 $\mu g\ m^{-3}$ (by 32.4%) during COVID-19 lockdown. The observed O_3 concentration, however, increases from 13.9 to 27.2 ppbv, almost doubling during COVID-19 lockdown.

2.2. Emission Setting

We use a two-way coupled Weather Research and Forecasting with Chemistry model (WRF-Chem v3.7) to simulate meteorology, gas, and aerosol concentrations simultaneously (Grell et al., 2005). The model configuration including natural emissions, and parameterization schemes are detailed in Text S2, and Table S1, respectively. Following P. Wang et al. (2020), we use Multi-resolution Emission Inventory for China

of 2016 (http://meicmodel.org/dataset-meic.html) as the basic anthropogenic emission inventory for the simulation period. It is noted that the emission change since 2016 will not affect the study significantly as the uncertainties of emission inventory usually surpass the emission changes over several year scales (Chen et al., 2014; Y. Zhao et al., 2011). We estimate the emission reductions owing to COVID-19 lockdown following Huang et al. (2020). The anthropogenic emissions of $PM_{2.5}$ and O_3 precursors summed over NCP are reduced by 8.3%–47.9% as a result of COVID-19 lockdown (Figure S2). Among all precursors, nitrogen oxides (NO_x) emissions exhibit the most significant decrease of 47.9% since most transportation is prohibited during COVID-19 lockdown.

2.3. Experimental Design

Four sensitivity simulations (ER_ARF, NoER_ARF, ER_NoARF, and NoER_NoARF) are conducted to examine how ARF affects the effectiveness of emission mitigation by conducting/no conducting emission reduction and with/without ARF during COVID-19 lockdown (Table S2). Experiment ER_ARF is designed to represent actual condition with emission reduction and ARF. The difference between ER_ARF and NoER_ARF shows the effects of emission reduction with ARF considered. The difference between ER_NoARF and NoER_NoARF indicates the effects of emission mitigation alone which do not consider the feedbacks between aerosol and meteorology. Therefore, the difference between (ER_ARF–NoER_ARF) and (ER_NoARF–NoER_NoARF) reflects the impact of ARF on the effectiveness of emission reduction during COVID-19 lockdown, which is the aim of this study. To further test how the effects of ARF on the effectiveness of emission control vary with emission reduction degrees, we conduct another series of sensitivity experiments with emission reductions in different degrees (Table S2). The difference between (iER_ARF–NoER_ARF) and (iER_NoARF–NoER_NoARF) represents the impact of ARF on the effectiveness of emission reduction in different degrees. The comparisons between simulations (in Experiment ER_ARF) and measurements (meteorological and environmental) are shown in Text S3 and Figures S3–S6.

2.4. Process Analysis

Integrated process rate (IPR) analysis, i.e., process analysis technique, is an advanced tool to quantitatively evaluate integrated rates of key processes simulated in the grid-based Eulerian models (J. Gao et al., 2018; Xing et al., 2017). Chen et al. (2019) developed an improved IPR scheme in the WRF-Chem model to separate the processes influencing pollutant variations into different processes, i.e., emission source (EMIS), advection (TRAN), subgrid convection (SGCV), vertical mixing (VMIX), wet scavenging (WETP), gas-phase chemistry (GASC), aerosol chemistry (AERC), and cloud chemistry (CLDC). Traditionally, the IPR analysis is conducted over one time step (e.g., 60 min). Therefore, the contribution of each process to pollutant change is usually quantified compared with previous hour. Based on Chen et al. (2019), we extend the use of IPR in this study to investigate the contribution of each physical/chemical process to pollutant change averaged over a period of time compared with another.

3. Results and Discussion

3.1. Effects of Emission Reduction on Meteorology

As shown in Figure S2, the anthropogenic emissions over NCP exhibit significant reductions as a result of COVID-19 lockdown, which leads to decreases in aerosol concentrations (Figure 2g). The variations in aerosols perturb radiative balance and further change meteorological conditions. Figure 1 shows the changes in meteorological variables, including downward shortwave radiative flux at the surface (SW_SUR) and in the atmosphere (SW_ATM), 2m temperature (T_2), 2m relative humidity (RH_2), 10m wind speed (WS_{10}), and PBLH, due to emission control during COVID-19 lockdown. The changes are calculated by subtracting the model results of NoER_ARF from those of ER_ARF.

The SW_SUR exhibits overall increases when emission reduction is enforced, with the largest increases occurring in southern Hebei. Generally, the SW_SUR averaged over NCP is enhanced by 2.3 W m^{-2} during

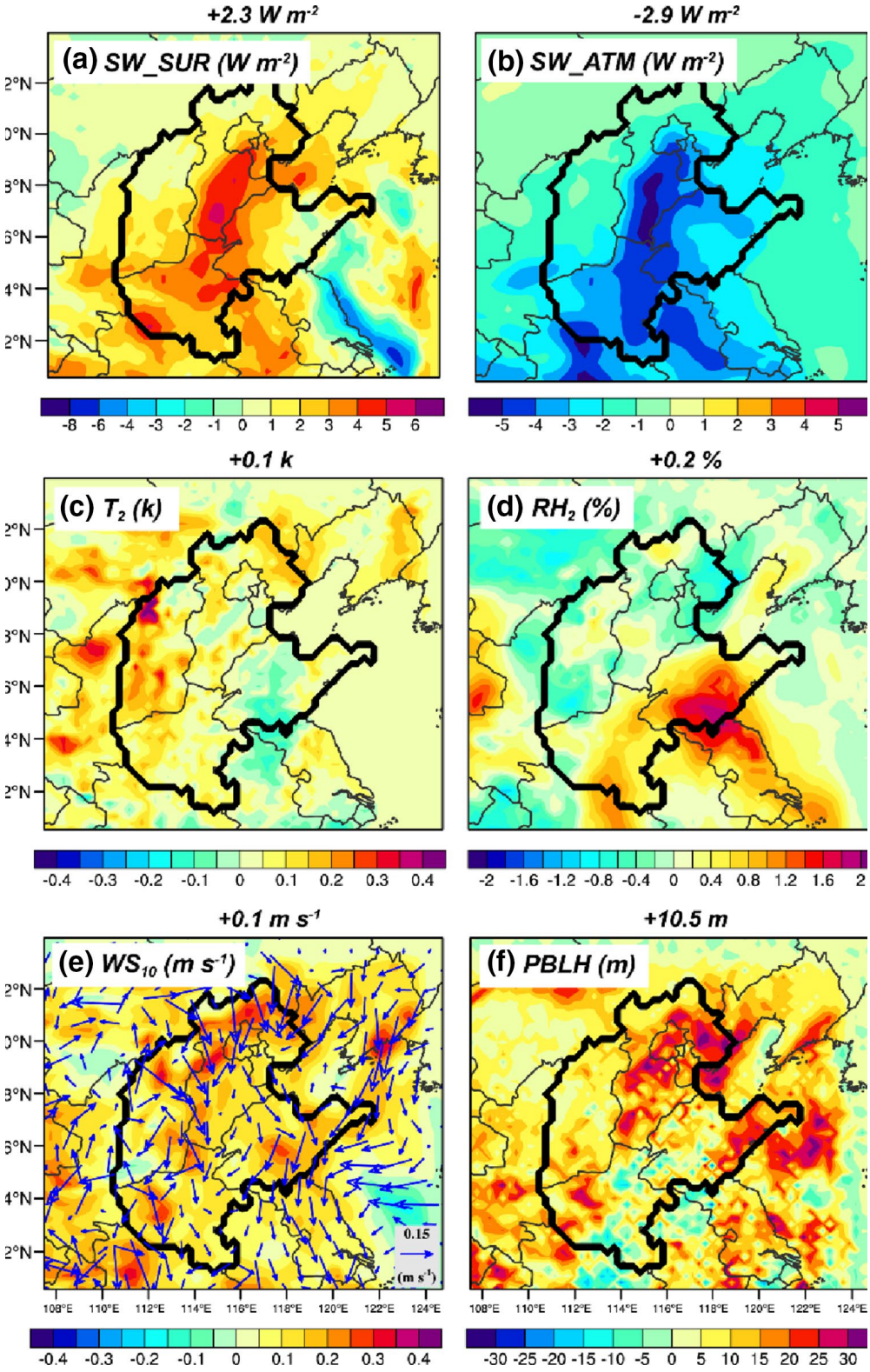

Figure 1. Changes in meteorological parameters due to emission control during COVID-19 lockdown. Meteorological variables include downward shortwave radiative flux (a) at the surface (SW_SUR) and (b) in the atmosphere (SW_ATM), (c) 2m temperature (T_2), (d) 2m relative humidity (RH_2), (e) 10m wind speed (WS_{10}), and (f) planetary boundary layer height (PBLH). Note that both the colored shading and arrow length represent wind speed, and arrow direction represents wind direction in (e). The changes averaged over North China Plain (NCP) are shown at the top of each panel.

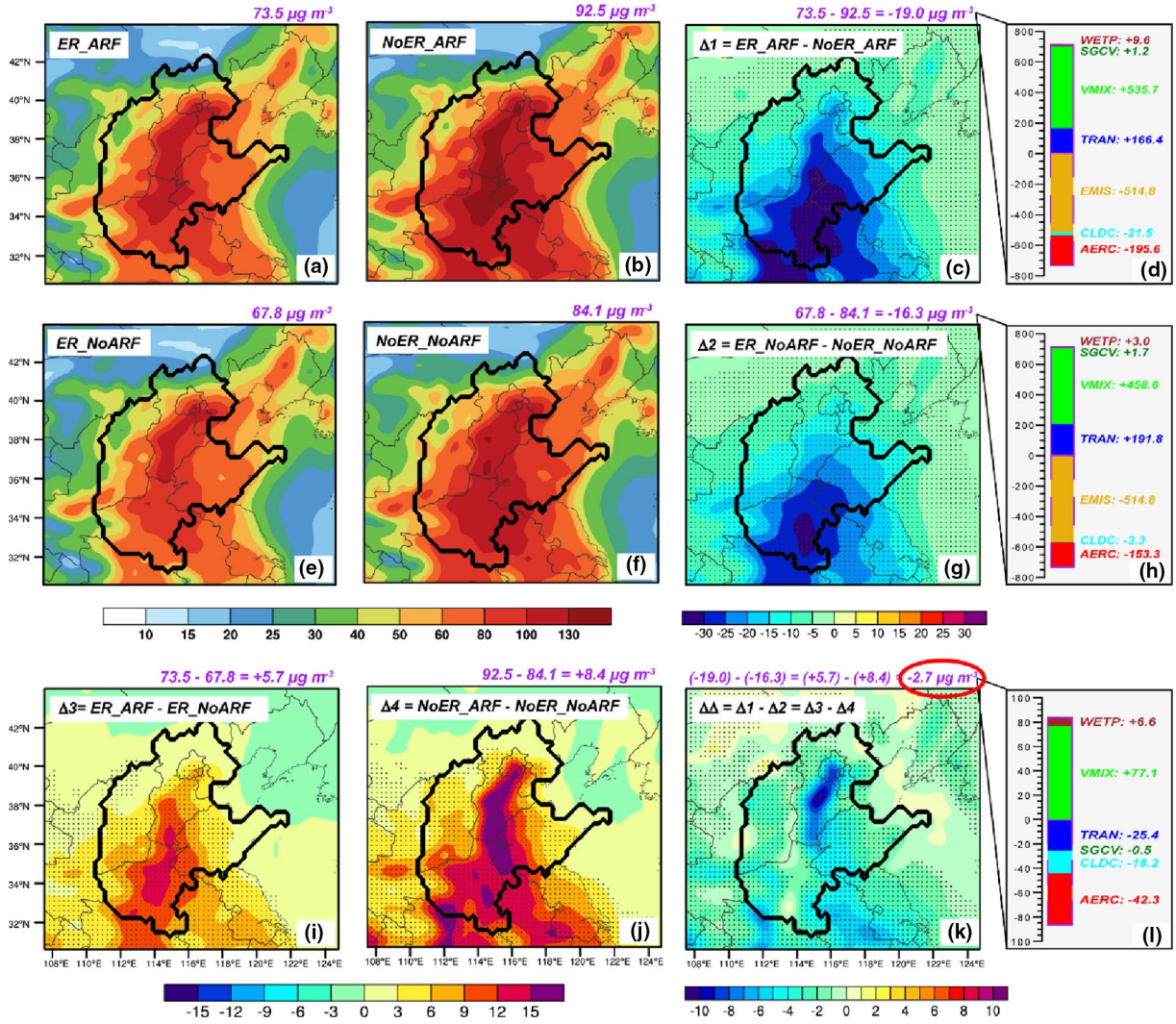

Figure 2. (a, b, e, and f) Spatial distributions of simulated $PM_{2.5}$ concentrations under four sensitivity simulations during COVID-19 lockdown. (i and j) Effects of aerosol-radiation feedback (ARF) on $PM_{2.5}$ concentrations under two emission scenarios. (c and g) Effects of emission reduction on $PM_{2.5}$ concentrations (c) with and (g) without ARF. (k) Effect of ARF on the effectiveness of emission reduction for $PM_{2.5}$ air quality. (d, h, and l) Contributions of each physical/chemical process to $PM_{2.5}$ changes. The (changed) $PM_{2.5}$ levels averaged over North China Plain (NCP) are shown at the top of each panel.

COVID-19 lockdown. X. Wen, Liu, et al. (2020) and Peters et al. (2020) provided observational evidences of increased solar radiation at the surface during COVID-19 outbreak over China and India, respectively. Contrary to the positive effect at the surface, the SW_ATM averaged over NCP decreases by 2.9 W m^{-2} as a result of emission control. It is well known that the existence of aerosol could reduce the SW_SUR but enhance SW_ATM due to aerosol scattering and absorption of solar radiation (Y. Gao et al., 2015; Qiu et al., 2017). Therefore, the lower aerosol concentrations owing to emission mitigation lead to positive changes for SW_SUR but negative changes for SW_ATM. Because the shortwave radiation reaching the ground is enhanced, near-surface temperature T_2 generally increases, with the average rise of 0.1 K over NCP and the maximum rise of 0.4 K in Shanxi. The RH_2 exhibits decreases over Beijing, Tianjin, Hebei, and Shanxi, resulting from the increase in saturation vapor pressure due to the increase in T_2 over these regions. The anomalous decreases in T_2 and increases in RH_2 occurring in Shandong result from the intensification of precipitation over the region (figure for precipitation is not shown). The warming due to increased SW_SUR and cooling due to decreased SW_ATM promote instability of atmosphere, which further accelerates near-surface wind speed and rises boundary layer. The WS_{10} and PBLH averaged over NCP increase by 0.1 m/s and 10.5 m, respectively. The increased northwesterly is simulated over NCP, which may influence the transport of $PM_{2.5}$ and O_3.

3.2. Effects of Emission Reduction on $PM_{2.5}$ Air Quality With Versus Without ARF

Figures 2a, 2b, 2e, and 2f show the spatial distributions of simulated $PM_{2.5}$ concentrations under four sensitivity simulations during COVID-19 lockdown. For each scenario, high $PM_{2.5}$ levels are all found over the analyzed region, with the largest concentrations in southern Hebei. Figures 2i and 2j exhibit the positive effects of ARF on $PM_{2.5}$ concentrations under two emission scenarios (shown by ER_ARF minus ER_NoARF and NoER_ARF minus NoER_NoARF, respectively). The radiative effects of aerosols lead to overall increases in $PM_{2.5}$ concentrations over NCP for each emission scenario. The aerosol-induced changes in meteorological variables (i.e., the cooling at the surface and the warming in the atmosphere, the more stable atmosphere, the increase in relative humidity at the surface, and the decrease in near-surface wind speed and PBLH) are beneficial for $PM_{2.5}$ production and accumulation in the lower atmosphere and therefore responsible for the significant increases of $PM_{2.5}$ levels. The positive feedback between aerosols and aerosol-induced meteorological conditions has been widely reported by previous studies (Huang et al., 2018; Liu et al., 2018; Su et al., 2018).

We place emphasis, in this study, on the effects of emission mitigation on $PM_{2.5}$ air quality with and without ARF. With ARF considered, the emission reduction due to COVID-19 lockdown leads to overall declines of $PM_{2.5}$ concentrations (Figure 2c). The averaged $PM_{2.5}$ level over the NCP decreases by 19.0 $\mu g\ m^{-3}$; the largest $PM_{2.5}$ reduction exceeds 30.0 $\mu g\ m^{-3}$ in Henan province. We further use the IPR analysis to examine the contribution of each physical/chemical process to $PM_{2.5}$ decrease. As shown in Figure 2d, the EMIS, AERC, and CLDC processes are responsible for the $PM_{2.5}$ decline. The primary emission of aerosol (EMIS) makes the largest contribution to the $PM_{2.5}$ decrease, followed by secondary transformation of aerosol (AERC and CLDC). On the contrary, the physical processes (e.g., VMIX and TRAN) exert an opposite effect on $PM_{2.5}$ changes. It's quite easy to understand the decreases induced by primary emission since strict emission control measures are implemented. The decreases in the chemical production of $PM_{2.5}$ (shown by AERC plus CLDC process) are mainly contributed by the declines in nitrate; instead, more sulfates are generated in response to the emission reduction (Figure S7). Le et al. (2020) conducted a model sensitivity simulation and reported that NO_x emission reduction would induce the reduction in nitrate aerosol but the increase in sulfate aerosol. The latter increase could be attributed to the promoted atmospheric oxidizing capacity. Huang et al. (2020) revealed that large decreases in NO_x emissions during COVID-19 lockdown increased O_3 and nighttime NO_3 radical formation, and the intensification in atmospheric oxidizing capacity in turn promoted formation of secondary aerosol.

When ARF is not considered, the emission reduction alone also results in overall $PM_{2.5}$ declines over NCP (Figure 2g). However, the $PM_{2.5}$ decreases without ARF are much weaker than those with ARF (Figure 2g vs. Figure 2c). The $PM_{2.5}$ concentration averaged over the NCP (without ARF) decreases by 16.3 $\mu g\ m^{-3}$ due to the COVID-19 restriction. The IPR analysis (Figure 2h) also reveals that the $PM_{2.5}$ decline is contributed by EMIS, AERC, and CLDC processes.

The effect of ARF on the effectiveness of emission reduction for $PM_{2.5}$ air quality can be quantified by the difference between the emission-reduction-induced $PM_{2.5}$ changes with and without ARF (Figure 2k). The consideration of ARF enhances $PM_{2.5}$ decreases all over the NCP. The largest enhancement of $PM_{2.5}$ decrease reaches 10.0 $\mu g\ m^{-3}$ in southern Hebei. Generally, the ARF enhances the emission-reduction-induced $PM_{2.5}$ decline by 2.7 $\mu g\ m^{-3}$ (16.6%) averaged over the NCP during COVID-19 lockdown. Further IPR analysis (Figure 2l) suggests that the ARF-induced enhancement of $PM_{2.5}$ decline is attributed to AERC, TRAN, and CLDC processes. The AERC makes the largest contribution, indicating that fewer aerosols are generated through aerosol chemistry process, which leads to the enhancement of $PM_{2.5}$ decline with ARF considered. The increased northwesterly (Figure 1e) brings low concentrations of $PM_{2.5}$ in northwestern China to NCP, accounting for the negative contribution from TRAN process.

3.3. Effects of Emission Reduction on O_3 Air Quality With Versus Without ARF

Aerosol-induced changes in meteorological conditions can also influence surface-layer O_3 concentrations by altering physical and chemical process. Figures 3i and 3j present the negative effects of ARF on O_3 concentrations under two emission scenarios. The radiative effects of aerosols result in overall decreases in O_3 concentrations over NCP under any emission scenario. Compared to the surface O_3 concentration without aerosol feedback, the surface O_3 concentration with ARF averaged over NCP declines by 2.1 and

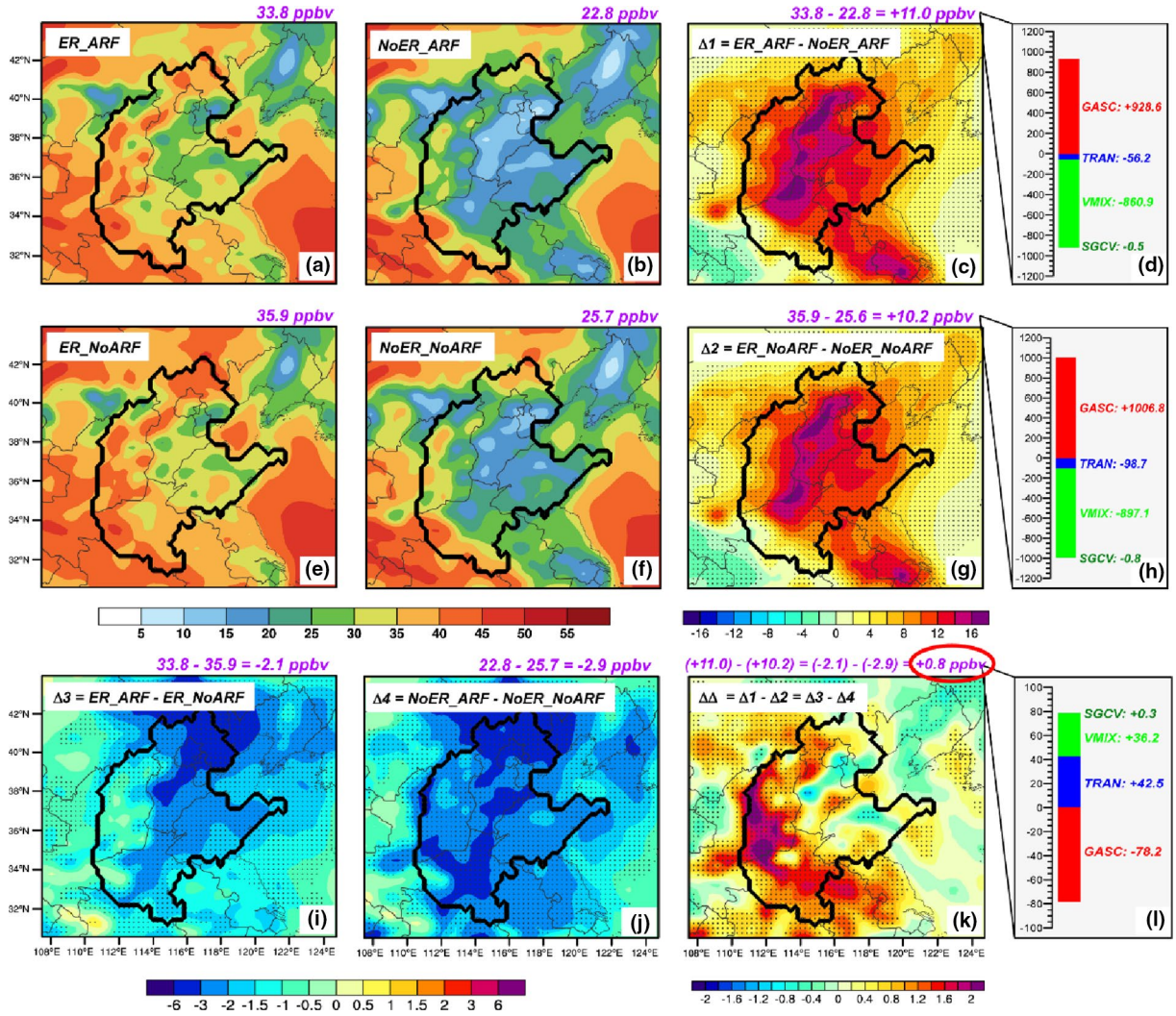

Figure 3. (a, b, e, and f) Spatial distributions of simulated O_3 concentrations under four sensitivity simulations during COVID-19 lockdown. (i and j) Effects of aerosol-radiation feedback (ARF) on O_3 concentrations under two emission scenarios. (c and g) Effects of emission reduction on O_3 concentrations (c) with and (g) without ARF. (k) Effect of ARF on the effectiveness of emission reduction for O_3 air quality. (d, h, and l) Contributions of each physical/chemical process to O_3 changes. The (changed) O_3 concentrations averaged over North China Plain (NCP) are shown at the top of each panel.

2.9 ppbv under two emission scenarios. Xing et al. (2017) also reported that aerosol-radiation effects reduced surface daily maxima 1 h O_3 over China by up to 39 $\mu g\ m^{-3}$ through the combination of changes in photolysis rates and changes in atmospheric dynamics in January of 2013.

We then focus intensively on the effects of emission reduction on O_3 air quality with and without ARF. With ARF considered, the emission control due to COVID-19 lockdown leads to overall increases of O_3 concentrations (Figure 3c). The averaged O_3 level over the NCP increases by 11.0 ppbv; the largest O_3 increase exceeds 16.0 ppbv in Hebei province. We further use the IPR analysis to quantify the contribution of each physical/chemical process to O_3 increase. As shown in Figure 3d, the GASC process accounts for the O_3 increase. On the contrary, the physical process (e.g., VMIX) exerts an opposite effect on O_3 change. During winter, the NCP is a VOC-limited region due to higher NO_x and lower biogenic VOC emissions (He, Zhang, et al., 2017; Leung et al., 2020). Under VOC-limited regime, NO_x reductions can relax OH depletion by NO_x and in turn produce more O_3; in addition, NO_x reductions can also increase O_3 by alleviating NO_x titration (Le et al., 2020; Leung et al., 2020). The $PM_{2.5}$ decrease could also be a factor for O_3 increase via the aerosol-photolysis interaction (G. Li, Bei, et al., 2017; Wu et al., 2020) as well as the reduced aerosol sink of hydroperoxy radicals (K. Li, Jacob, Liao, Shen, et al., 2019; K. Li, Jacob, Liao, Zhu, et al., 2019).

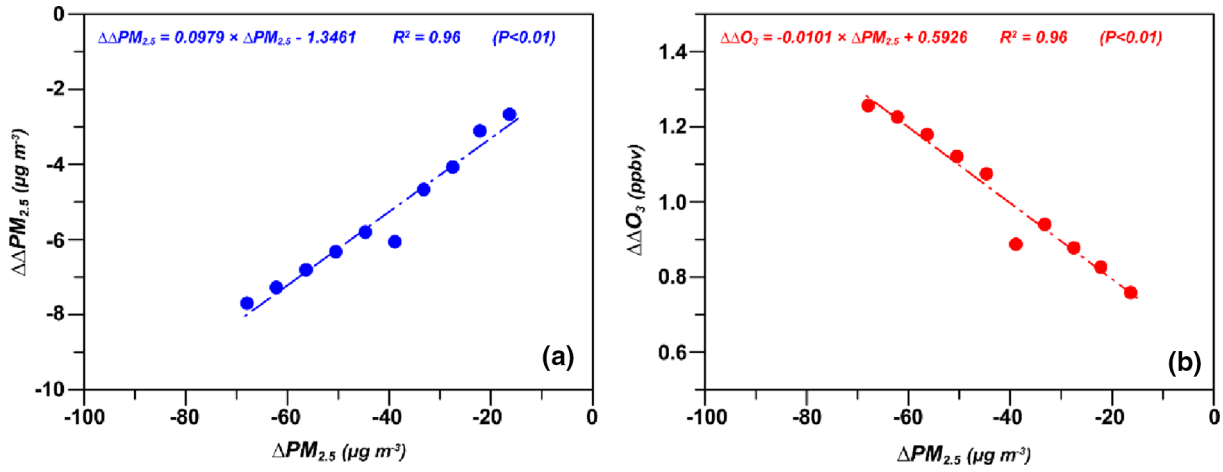

Figure 4. Relationships between emission-reduction-induced $PM_{2.5}$ decrease without ARF ($\Delta PM_{2.5}$) and ARF-induced enhancement of (a) $PM_{2.5}$ decrease ($\Delta\Delta PM_{2.5}$) and (b) O_3 increase ($\Delta\Delta O_3$). Linear fitting equations are shown at the top of each panel.

When ARF is excluded, the emission reduction alone also leads to overall O_3 increases over NCP (Figure 3g). However, the O_3 increases without ARF are weaker than those with ARF (Figure 3g vs. Figure 3c). The O_3 concentration averaged over the NCP (without ARF) rises by 10.2 ppbv in response to the COVID-19 restriction. Further IPR analysis (Figure 3h) also suggests that the GASC process contributes to the O_3 increase.

The impact of ARF on the effectiveness of emission reduction for O_3 air quality can be quantified by the difference between the emission-reduction-induced O_3 changes with and without ARF. The consideration of ARF enhances O_3 increases over most of NCP and weakens O_3 increases over a small fraction of the region (Figure 3k). The largest enhancement of O_3 increase exceeds 2.0 ppbv in Shanxi. On average, the ARF enhances the emission-reduction-induced O_3 increase by 0.8 ppbv (7.8%) over the NCP region during COVID-19 lockdown. We conduct further IPR analysis in Figure 3l and find that the ARF-induced enhancement of O_3 increase is attributed to TRAN and VMIX processes. The increased northwesterly (Figure 1e) brings high concentrations of O_3 in northwestern China to NCP, accounting for the positive contribution from TRAN process. With the development of PBL (Figure 1f), more O_3 are transported downward from the upper atmosphere to the near surface, leading to the increases in surface-layer O_3 levels (Chen et al., 2020; He, Gong, et al., 2017) contributed by VMIX process.

3.4. Relations Between Aerosol Changes and ARF Impacts

As described above, the emission reduction alone during COVID-19 lockdown induces $PM_{2.5}$ decrease by 16.3 μg m^{-3} averaged over NCP and the consideration of ARF enhances $PM_{2.5}$ decrease by 2.7 μg m^{-3}, leading to the net $PM_{2.5}$ decrease by 19.0 μg m^{-3}. That is, a model without ARF (i.e., offline model) will considerably underestimate emission-reduction-induced $PM_{2.5}$ decline by 16.6%. We further conduct a set of sensitivity experiments with emission reductions in different degrees to test the relationship between the $PM_{2.5}$ decrease induced by emission control alone and the enhancement of $PM_{2.5}$ decrease contributed by ARF. As presented by Figure 4a, the ARF-induced enhancement of $PM_{2.5}$ decrease shows a robust linear relationship ($R^2 = 0.96$, statistically significant at 99% confidence level) with the emission-reduction-induced $PM_{2.5}$ decrease without ARF. The stronger the abatement actions are, the greater the $PM_{2.5}$ improvement enhanced by ARF is.

As for O_3 air quality, the emission reduction alone during COVID-19 lockdown leads to a significant O_3 increase of 10.2 ppbv averaged over NCP and the consideration of ARF enhances O_3 increase by 0.8 ppbv, leading to the net O_3 increase by 11.0 ppbv. This indicates offline models without ARF will underestimate emission-control-induced O_3 rise by 7.8%. The sensitivity experiments with varying emission reductions indicate a statistically significant linear relationship ($R^2 = 0.96$) between the emission-reduction-induced $PM_{2.5}$ decrease without ARF and the enhancement of O_3 increase contributed by ARF (Figure 4b).

The fitted linear relationships have an important implication for assessing the effectiveness of emission abatement at any extent, and also provide offline models in the absence of ARF with an enforceable scheme to quantify the influence of ARF on the effectiveness of emission abatement and further estimate the net $PM_{2.5}$ or O_3 changes with ARF considered in response to emission reduction in any degree.

4. Conclusions

We use an online-coupled model WRF-Chem to examine ARF effects on $PM_{2.5}$ and O_3 responses to emission reduction during COVID-19 lockdown over NCP of China. The emission reduction alone induces $PM_{2.5}$ decrease by 16.3 $\mu g\ m^{-3}$; the ARF enhances $PM_{2.5}$ decrease by 2.7 $\mu g\ m^{-3}$ (16.6%), which is mainly attributed to aerosol chemistry process. For O_3, the increase of 10.2 ppbv caused by emission reduction alone is enhanced by 0.8 ppbv (7.8%) through ARF, which is ascribed to physical advection and vertical mixing processes. Beyond this, we extend our result for the COVID-19 case study to consider a set of emission reduction scenarios, and find that the ARF-induced enhancement of $PM_{2.5}$ decline (O_3 rise) linearly responses to emission-reduction-induced $PM_{2.5}$ decrease. However, whether the fitted relationship for wintertime applies to summer condition remains unknown, which needs to be verified through further sensitivity experiments for summertime in future studies. In addition, the weakened ARF due to improved $PM_{2.5}$ air quality since China's clean air actions would contribute to worsening O_3 pollution; quantitatively evaluating the contributions from weakened ARF will have an important implication for understanding rising O_3 levels over China since 2013, which is another following topic of great interest.

Data Availability Statement

Meteorological measurements from NOAA's National Climatic Data Center are publicly available at https://www.ncei.noaa.gov/data/global-hourly/access/2020/. Observed $PM_{2.5}$ and O_3 concentrations from China National Environmental Monitoring Centre can be obtained from https://met.iap.ac.cn/data/openaq/CN/. Multi-resolution Emission Inventory for China can be accessed publicly from http://meicmodel.org/dataset-meic.html, and the emission reduction ratios due to COVID-19 lockdown are available from Table S1 at https://academic.oup.com/nsr/advance-article/doi/10.1093/nsr/nwaa137/5859289. Model results are available at https://zenodo.org/record/4059188#.X3Q5EWgzabh. The authors declare no conflict of interest.

Acknowledgments
This work is supported by the National Key R&D Program of China (2019YFA0606804), the National Natural Science Foundation of China (42007195), and the University Natural Science Research Foundation of Jiangsu Province (18KJB170012).

References

Chen, L., Sun, Y., Wu, X., Zhang, Y., Zheng, C., Gao, X., & Cen, K. (2014). Unit-based emission inventory and uncertainty assessment of coal-fired power plants. *Atmospheric Environment*, *99*, 527–535. https://doi.org/10.1016/j.atmosenv.2014.10.023

Chen, L., Zhu, J., Liao, H., Gao, Y., Qiu, Y., Zhang, M., et al. (2019). Assessing the formation and evolution mechanisms of severe haze pollution in the Beijing–Tianjin–Hebei region using process analysis. *Atmospheric Chemistry and Physics*, *19*(16), 10845–10864. https://doi.org/10.5194/acp-19-10845-2019

Chen, L., Zhu, J., Liao, H., Yang, Y., & Yue, X. (2020). Meteorological influences on $PM_{2.5}$ and O_3 trends and associated health burden since China's clean air actions. *Science of the Total Environment*, *744*, 140837. https://doi.org/10.1016/j.scitotenv.2020.140837

Gao, M., Liu, Z., Wang, Y., Lu, X., Ji, D., Wang, L., et al. (2017). Distinguishing the roles of meteorology, emission control measures, regional transport, and co-benefits of reduced aerosol feedbacks in "APEC Blue". *Atmospheric Environment*, *167*, 476–486. https://doi.org/10.1016/j.atmosenv.2017.08.054

Gao, Y., Zhang, M., Liu, Z., Wang, L., Wang, P., Xia, X., et al. (2015). Modeling the feedback between aerosol and meteorological variables in the atmospheric boundary layer during a severe fog-haze event over the North China Plain. *Atmospheric Chemistry and Physics*, *15*(8), 4279–4295. https://doi.org/10.5194/acp-15-4279-2015

Gao, J., Zhu, B., Xiao, H., Kang, H., Pan, C., Wang, D., & Wang, H. (2018). Effects of black carbon and boundary layer interaction on surface ozone in Nanjing, China. *Atmospheric Chemistry and Physics*, *18*(10), 7081–7094. https://doi.org/10.5194/acp-18-7081-2018

Grell, G. A., Peckham, S. E., Schmitz, R., McKeen, S. A., Frost, G., Skamarock, W. C., & Eder, B. (2005). Fully coupled "online" chemistry within the WRF model. *Atmospheric Environment*, *39*(37), 6957–6975. https://doi.org/10.1016/j.atmosenv.2005.04.027

He, J., Gong, S., Yu, Y., Yu, L., Wu, L., Mao, H., et al. (2017). Air pollution characteristics and their relation to meteorological conditions during 2014–2015 in major Chinese cities. *Environmental Pollution*, *223*, 484–496. https://doi.org/10.1016/j.envpol.2017.01.050

He, J., Zhang, Y., Wang, K., Chen, Y., Leung, L. R., Fan, J., et al. (2017). Multi-year application of WRF-CAM5 over East Asia-Part I: Comprehensive evaluation and formation regimes of O_3 and $PM_{2.5}$. *Atmospheric Environment*, *165*, 122–142. https://doi.org/10.1016/j.atmosenv.2017.06.015

Huang, X., Ding, A., Gao, J., Zheng, B., Zhou, D., Qi, X., et al. (2020). Enhanced secondary pollution offset reduction of primary emissions during COVID-19 lockdown in China. *National Science Review*, nwaa137. https://doi.org/10.1093/nsr/nwaa137

Huang, X., Wang, Z., & Ding, A. (2018). Impact of aerosol-PBL interaction on haze pollution: Multiyear observational evidences in North China. *Geophysical Research Letters*, *45*(16), 8596–8603. https://doi.org/10.1029/2018gl079239

Leung, D. M., Shi, H., Zhao, B., Wang, J., Ding, E. M., Gu, Y., et al. (2020). Wintertime particulate matter decrease buffered by unfavorable chemical processes despite emissions reductions in China. *Geophysical Research Letters*, *47*(14). https://doi.org/10.1029/2020GL087721

Le, T., Wang, Y., Liu, L., Yang, J., Yung, Y. L., Li, G., & Seinfeld, J. H. (2020). Unexpected air pollution with marked emission reductions during the COVID-19 outbreak in China. *Science*, *369*(6504), 702–706. https://doi.org/10.1126/science.abb7431

Li, G., Bei, N., Cao, J., Wu, J., Long, X., Feng, T., et al. (2017). Widespread and persistent ozone pollution in eastern China during the non-winter season of 2015: Observations and source attributions. *Atmospheric Chemistry and Physics*, *17*(4), 2759–2774. https://doi.org/10.5194/acp-17-2759-2017

Li, Z., Guo, J., Ding, A., Liao, H., Liu, J., Sun, Y., et al. (2017). Aerosol and boundary-layer interactions and impact on air quality. *National Science Review*, *4*(6), 810–833. https://doi.org/10.1093/nsr/nwx117

Li, J., Han, Z., Wu, Y., Xiong, Z., Xia, X., Li, J., et al. (2020). Aerosol radiative effects and feedbacks on boundary layer meteorology and $PM_{2.5}$ chemical components during winter haze events over the Beijing-Tianjin-Hebei region. *Atmospheric Chemistry and Physics*, *20*, 8659–8690. https://doi.org/10.5194/acp-20-8659-2020

Li, J., Han, Z., Yao, X., Xie, Z., & Tan, S. (2019). The distributions and direct radiative effects of marine aerosols over East Asia in springtime. *Science of the Total Environment*, *651*, 1913–1925. https://doi.org/10.1016/j.scitotenv.2018.09.368

Li, K., Jacob, D. J., Liao, H., Shen, L., Zhang, Q., & Bates, K. H. (2019). Anthropogenic drivers of 2013–2017 trends in summer surface ozone in China. *Proceedings of the National Academy of Sciences of the United States of America*, *116*(2), 422–427. https://doi.org/10.1073/pnas.1812168116

Li, K., Jacob, D. J., Liao, H., Zhu, J., Shah, V., Shen, L., et al. (2019). A two-pollutant strategy for improving ozone and particulate air quality in China. *Nature Geoscience*, *12*, 906–910. https://doi.org/10.1038/s41561-019-0464-x

Li, Z., Rosenfeld, D., & Fan, J. (2017). Aerosols and their impact on radiation, clouds, precipitation, and severe weather events. In *Oxford Research Encyclopedias*. https://doi.org/10.1093/acrefore/9780199389414.013.126

Liu, Q., Jia, X., Quan, J., Li, J., Li, X., Wu, Y., et al. (2018). New positive feedback mechanism between boundary layer meteorology and secondary aerosol formation during severe haze events. *Scientific Reports*, *8*(1), 6095. https://doi.org/10.1038/s41598-018-24366-3

Lou, S., Russell, L. M., Yang, Y., Liu, Y., Singh, B., & Ghan, S. J. (2017). Impacts of interactive dust and its direct radiative forcing on interannual variations of temperature and precipitation in winter over East Asia. *Journal of Geophysical Research: Atmospheres*, *122*(16), 8761–8780. https://doi.org/10.1002/2017JD027267

Lou, S., Yang, Y., Wang, H., Smith, S. J., Qian, Y., & Rasch, P. J. (2019). Black carbon amplifies haze over the North China Plain by weakening the East Asian winter monsoon. *Geophysical Research Letters*, *46*(1), 452–460. https://doi.org/10.1029/2018GL080941

Petaja, T., Jarvi, L., Kerminen, V. M., Ding, A. J., Sun, J. N., Nie, W., et al. (2016). Enhanced air pollution via aerosol-boundary layer feedback in China. *Scientific Reports*, *6*, 18998. https://doi.org/10.1038/srep18998

Peters, I. M., Brabec, C., Buonassisi, T., Hauch, J., & Nobre, A. M. (2020). The impact of COVID-19 related measures on the solar resource in areas with high levels of air pollution. *Joule*, *4*(8), 1681–1687. https://doi.org/10.1016/j.joule.2020.06.009

Qiu, Y., Liao, H., Zhang, R., & Hu, J. (2017). Simulated impacts of direct radiative effects of scattering and absorbing aerosols on surface layer aerosol concentrations in China during a heavily polluted event in February 2014. *Journal of Geophysical Research: Atmospheres*, *122*(11), 5955–5975. https://doi.org/10.1002/2016jd026309

Shi, X., & Brasseur, G. P. (2020). The response in air quality to the reduction of Chinese economic activities during the COVID-19 outbreak. *Geophysical Research Letters*, *47*. https://doi.org/10.1029/2020GL088070

Su, T., Li, Z., & Kahn, R. (2018). Relationships between the planetary boundary layer height and surface pollutants derived from lidar observations over China: Regional pattern and in fluencing factors. *Atmospheric Chemistry and Physics*, *18*(21), 15921–15935. https://doi.org/10.5194/acp-18-15921-2018

Tian, R., Ma, X., Jia, H., Yu, F., Sha, T., & Zan, Y. (2019). Aerosol radiative effects on tropospheric photochemistry with GEOS-Chem simulations. *Atmospheric Environment*, *208*, 82–94. https://doi.org/10.1016/j.atmosenv.2019.03.032

Wang, P., Chen, K., Zhu, S., Wang, P., & Zhang, H. (2020). Severe air pollution events not avoided by reduced anthropogenic activities during COVID-19 outbreak. *Resources, Conservation and Recycling*, *158*, 104814. https://doi.org/10.1016/j.resconrec.2020.104814

Wang, W., Li, X., Shao, M., Hu, M., Zeng, L., Wu, Y., & Tan, T. (2019). The impact of aerosols on photolysis frequencies and ozone production in Beijing during the 4-year period 2012–2015. *Atmospheric Chemistry and Physics*, *19*(14), 9413–9429. https://doi.org/10.5194/acp-19-9413-2019

Wen, W., Guo, C., Ma, X., Zhao, X., Chen, D., & Xu, J. (2020). Impact of emission reduction on aerosol-radiation interaction during heavy pollution periods over Beijing-Tianjin-Hebei region in China. *Journal of Environmental Sciences*, *95*, 2–13. https://doi.org/10.1016/j.jes.2020.03.025

Wen, X., Liu, C., Cao, B., Wang, S., Zhang, Y., & Zhong, R. (2020). Relationship between the COVID-19 outbreak and temperature, humidity, and solar radiation across China. *SSRN*. http://dx.doi.org/10.2139/ssrn.3594115

Wu, J., Bei, N., Hu, B., Liu, S., Wang, Y., Shen., Z., et al. (2020). Aerosol–photolysis interaction reduces particulate matter during wintertime haze events. *Proceedings of the National Academy of Sciences of the United States of America*, *117*(18), 9755–9761. https://doi.org/10.1073/pnas.1916775117

Xing, J., Mathur, R., Pleim, J., Hogrefe, C., Gan, C. M., Wong, D. C., et al. (2015). Air pollution and climate response to aerosol direct radiative effects: A modeling study of decadal trends across the northern hemisphere. *Journal of Geophysical Research: Atmospheres*, *120*(23), 12221–12236. https://doi.org/10.1002/2015JD023933

Xing, J., Wang, J., Mathur, R., Wang, S., Sarwar, G., Pleim, J., et al. (2017). Impacts of aerosol direct effects on tropospheric ozone through changes in atmospheric dynamics and photolysis rates. *Atmospheric Chemistry and Physics*, *17*(16), 9869–9883. https://doi.org/10.5194/acp-17-9869-2017

Yang, Y., Russell, L. M., Lou, S., Liao, H., Guo, J., Liu, Y., et al. (2017). Dust-wind interactions can intensify aerosol pollution over eastern China. *Nature Communications*, *8*(1), 15333. https://doi.org/10.1038/ncomms15333

Zhao, B., Liou, K. N., Gu, Y., Li, Q., Jiang, J. H., Su, H., et al. (2017). Enhanced $PM_{2.5}$ pollution in China due to aerosol-cloud interactions. *Scientific Reports*, *7*(1), 4453. https://doi.org/10.1038/s41598-017-04096-8

Zhao, Y., Nielsen, C. P., Lei, Y., McElroy, M. B., & Hao, J. (2011). Quantifying the uncertainties of a bottom-up emission inventory of anthropogenic atmospheric pollutants in China. *Atmospheric Chemistry and Physics*, *11*(5), 2295–2308. https://doi.org/10.5194/acp-11-2295-2011

Zhao, Y., Zhang, K., Xu, X., Shen, H., Zhu, X., Zhang, Y., et al. (2020). Substantial changes in nitrogen dioxide and ozone after excluding meteorological impacts during the COVID-19 outbreak in mainland China. *Environmental Science & Technology Letters*, *7*(6), 402–408. https://doi.org/10.1021/acs.estlett.0c00304

Zhou, M., Zhang, L., Chen, D., Gu, Y., Fu, T.-M., Gao, M., et al. (2019). The impact of aerosol-radiation interactions on the effectiveness of emission control measures. *Environmental Research Letters*, *14*(2), 024002. https://doi.org/10.1088/1748-9326/aaf27d

Zhu, J., Chen, L., Liao, H., & Dang, R. (2019). Correlations between $PM_{2.5}$ and ozone over China and associated underlying reasons. *Atmosphere*, *10*(7), 352. https://doi.org/10.3390/atmos10070352

References From the Supporting Information

Chen, L., Zhang, M., Zhu, J., Wang, Y., & Skorokhod, A. (2018). Modeling impacts of urbanization and urban heat island mitigation on boundary layer meteorology and air quality in Beijing under different weather conditions. *Journal of Geophysical Research: Atmospheres*, *123*(8), 4323–4344. https://doi.org/10.1002/2017jd027501

Gao, M., Liu, Z., Zheng, B., Ji, D., Sherman, P., Song, S., et al. (2020). China's emission control strategies have suppressed unfavorable influences of climate on wintertime $PM_{2.5}$ concentrations in Beijing since 2002. *Atmospheric Chemistry and Physics*, *20*(3), 1497–1505. https://doi.org/10.5194/acp-20-1497-2020

Gong, S. L., Barrie, L. A., & Blanchet, J. P. (1997). Modeling sea-salt aerosols in the atmosphere: 1. Model development. *Journal of Geophysical Research*, *102*, 3805–3818. https://doi.org/10.1029/96jd02953

Guenther, A., Karl, T., Harley, P., Wiedinmyer, C., Palmer, P. I., & Geron, C. (2006). Estimates of global terrestrial isoprene emissions using MEGAN (Model of Emissions of Gases and Aerosols from Nature). *Atmospheric Chemistry and Physics*, *6*, 3181–3210. https://doi.org/10.5194/acp-6-3181-2006

Marsh, D. R., Mills, M. J., Kinnison, D. E., Lamarque, J. F., Calvo, N., & Polvani, L. M. (2013). Climate change from 1850 to 2005 simulated in CESM1 (WACCM). *Journal of Climate*, *26*(19), 7372–7391. https://doi.org/10.1175/jcli-d-12-00558.1

Qiu, Y., Ma, Z., & Li, K. (2019). A modeling study of the peroxyacetyl nitrate (PAN) during a wintertime haze event in Beijing, China. *Science of the Total Environment*, *650*, 1944–1953. https://doi.org/10.1016/j.scitotenv.2018.09.253

Shao, Y. (2004). Simplification of a dust emission scheme and comparison with data. *Journal of Geophysical Research*, *109*(D10), D10202. https://doi.org/10.1029/2003jd004372

van der Werf, G. R., Randerson, J. T., Giglio, L., Collatz, G. J., Mu, M., Kasibhatla, P. S., et al. (2010). Global fire emissions and the contribution of deforestation, savanna, forest, agricultural, and peat fires (1997–2009). *Atmospheric Chemistry and Physics*, *10*, 11707–11735. https://doi.org/10.5194/acp-10-11707-2010

Zhang, B., Wang, Y., & Hao, J. (2015). Simulating aerosol–radiation–cloud feedbacks on meteorology and air quality over eastern China under severe haze conditions in winter. *Atmospheric Chemistry and Physics*, *15*(5), 2387–2404. https://doi.org/10.5194/acp-15-2387-2015